

FINO-Net: A Deep Multimodal Sensor Fusion Framework for Manipulation Failure Detection

Arda Inceoglu¹, Eren Erdal Aksoy², Abdullah Cihan Ak¹, Sanem Sariel¹

Abstract—Safe manipulation in unstructured environments for service robots is a challenging problem. A failure detection system is needed to monitor and detect unintended outcomes. We propose FINO-Net, a novel multimodal sensor fusion based deep neural network to detect and identify manipulation failures. We also introduce a multimodal dataset, containing 229 real-world manipulation data recorded with a Baxter robot. Our network combines RGB, depth and audio readings to effectively detect and classify failures. Results indicate that fusing RGB with depth and audio modalities significantly improves the performance. FINO-Net achieves %98.60 detection and %87.31 classification accuracy on our novel dataset. Code and data are publicly available at <https://github.com/ardai/fin-net>.

I. INTRODUCTION

The use of service robots in domestic environments raises some important ethical concerns which must be taken into account in robot designs. One crucial concern is execution safety in such environments where robots work with humans and everyday objects. Although robots are equipped with well designed actions, unintended or unsafe situations may arise from failed executions of these actions in the real world due to either faults in perception, failures in actuation or unforeseen events. Physical interactions with objects may result in collisions, fall downs, spills or overturnings. Robots should monitor these types of interactions to protect objects in interaction, humans in collaboration, themselves, and their environments.

The primary step in execution safety is to be equipped with essential skills to detect failures or unsafe situations. After then, predictions and precautions are possible. Execution monitoring and safety has been a well investigated research area [1], [2] and several methods exist for both ground and aerial robots [3]–[5]. However, there still exist several research questions for service robots working in unstructured environments. This is the main motivation behind our work. We investigate how robots can effectively detect and identify manipulation failures as a first step in safe execution. We define a *failure* as an unintended outcome of an action execution. Sample failures that we focus on a selected

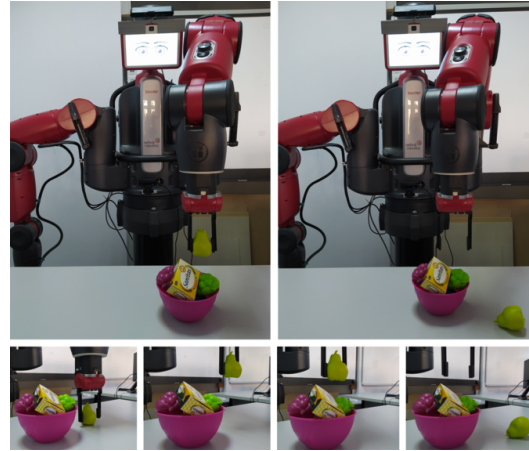


Fig. 1: Snapshots from a failed put-in-container execution.

primitive tabletop manipulation action set: *push*, *pick&place*, *put-in*, *put-on*, and *pour*. A sample *put-in* execution failure of our humanoid robot is given in Fig. 1. The robot fails in putting a plastic pear into a bowl full of other items.

It is almost impossible to detect and identify failures without perception. Furthermore, multi sensory integration is more desirable to take advantages of each sensor’s perceptual contribution [6]. Multimodal sensor fusion methods are extensively used for manipulation, and execution monitoring also benefits from the use of multimodal data [7]–[10]. However, there exist potential challenges to deal with multimodal sensor fusion: (i) different data formats, (ii) different operating regimes/frequencies, (iii) inter and/or intra conflicting observations of sensors.

To address the above mentioned challenges, we propose a deep multimodal sensor fusion framework for manipulation failure detection and identification, Failure Is Not an Option (FINO)-Net. The framework effectively detects and classifies manipulation failures by fusing visual (RGB and depth) and audio modalities. Our framework adopts early fusion to combine RGB and depth frames and late fusion to combine vision and audio data. To capture spatio-temporal features in sensory observations, modalities are processed individually with a series of convolutional and convolutional-LSTM layers, then the latent space representations are combined for detection and classification.

Our earlier work involves an analysis on contributions of different sensor modalities on failure detection [11]. Based on this analysis, we developed a Hidden Markov Model-based failure detection system where the features are collected through classifiers [12]. Our new FINO-Net frame-

¹Artificial Intelligence and Robotics Laboratory, Faculty of Computer and Informatics Engineering, Istanbul Technical University, Maslak, Turkey {inceoglu, akab, sariel}@itu.edu.tr

²School of Information Technology, Center for Applied Intelligent Systems Research, Halmstad University, Halmstad, Sweden eren.aksoy@hh.se

At this work, Arda Inceoglu was supported by the Turkcell-Istanbul Technical University Researcher Funding Program. We gratefully acknowledge the support of NVIDIA Corporation with the donation of the Quadro P6000 GPU used for this research. This research is also supported by a grant from the Scientific and Technological Research Council of Turkey (TUBITAK), Grant No. 119E-436.

work uses the same modalities as input. However, it does not rely on precomputed features but rather processes raw sensory data in an end-to-end manner for failure detection and identification.

The main contributions of this paper are as follows:

- We introduce a novel deep neural network model that fuses multimodal sensory readings to detect and identify possible failure types.
- We further analyze the unique contribution of each sensing modality on the failure detection and identification tasks.
- We release a multimodal (RGB, depth and audio) real-world dataset of 5 different manipulation types with in total 229 manipulation scenarios. We evaluate the performance of FINO-Net on this dataset.

II. RELATED WORK

We first review the earlier literature on failure detection, execution monitoring, and multimodal sensor fusion. We then discuss some previously published manipulation datasets and elaborate on why we need to introduce our own new dataset.

A. Failure Detection and Execution Monitoring

In the literature, *failure* (a.k.a *fault* or *anomaly*) *detection* and *execution monitoring* keywords are used interchangeably. The work in [13] summarizes deep learning based anomaly detection for various application domains. From the robotics perspective, there are model-based and model-free approaches proposed for execution monitoring [14]. The former approach compares the already known models with observations, whereas the latter uses sensory observation to make predictions [1], [2].

Among earlier model-based approaches, Kalman Filter (KF) [3], kinematic model [4], and residual [5] based systems are proposed to detect and identify mechanical and sensor failures. Execution models [15] and stochastic action models [16] are used to detect and correct [17] execution anomalies. In [18] action models are extended to detect and recover from failures by repairing the plan. Additionally, Description Logic (DL) [19], Temporal Action Logic (TAL) [20] and Metric Temporal Logic (MTL) [7] formulas are defined for execution monitoring. Furthermore, the work in [21] uses a domain-specific language based approach to monitor software components.

On the other hand, model-free execution monitoring methods employ pattern recognition techniques [22]. The recent work in [23] extends planning with a vision-based execution monitoring system to search for target objects in the scene to ensure planning pre-conditions are satisfied. In [24] different preprocessing techniques for introspective data are analysed to detect gearbox failures for industrial robot arms. Non-parametric bayesian models are proposed for execution monitoring in robotics [25]. Non-parametric Hidden Markov Models (HMMs) representing spatio-temporal dynamics of anomalies are applied in [26] to detect and classify anomalies by considering only introspective data (i.e., force-torque, velocity, tactile). The method is evaluated on pick&place

tasks by using 6 varying sized and shaped objects on a Baxter robot. A multimodal execution monitoring system is proposed for the assistive feeding task in [8]. The authors adopt LSTM-based Variational Autoencoder to process multimodal input from camera, microphone, joint encoder, force sensor. In their earlier work, multivariate Gaussian HMMs are also explored [9].

Our work differs from the existing studies as we address the problem of detection and identification of manipulation failures which are mainly caused by the uncertainties in perception and execution. Unlike the works in [8], [9], where the focus is rather on the failures emerge during human-robot interaction (e.g. failures due to collision, face occlusion, utensil miss, user miss, sound from user, etc.), we investigate the robot-object interaction failures observed over the course of a manipulation. Instead of hand-crafted features such as sound energy, spoon position, and mouth position used in [8], [9], our proposed perception framework learns feature representations directly from the raw multimodal sensory data in an end-to-end fashion.

B. Multimodal Sensor Fusion

Multimodal fusion has wide variety of applications with different kind of input modalities [27]. The work in [28] fuses RGB and depth images for object recognition. RGB-D and audio are combined in [29] for human manipulation action recognition. In [7], RGB-D camera, sonar, microphone and tactile sensors are integrated, via high level predicates extracted from sensory data, in order to detect different kind of execution failures for mobile robots.

One of the main issues in multimodal sensor fusion is when unimodal data should be combined. Prior works introduce early, intermediate and late fusion based architectures. Early fusion combines low-level features (i.e., raw observations), whereas late fusion incorporates high-level features (i.e., close to prediction). In addition, intermediate architectures, where both early and late fusions are intertwined, rather cover different strategies to fuse intermediate-level features. Variety of network architectures are summarized in [30]. In this work, we adopt a combination of early and late fusion methods to combine different sensing modalities.

C. Manipulation Datasets

Recently, there have been great efforts to collect large scale robot manipulation data. These efforts, however, center around manipulation skill learning task and ignore failures emerge during manipulation executions. RoboTurk [31], [32] is a crowdsourced simulation tool to collect teleoperated manipulation data for imitation learning. The dataset also includes real robot RGB-D frames for the following tasks: object search, tower stacking and laundry layout. RoboNet [33] provides 15 million video frames, from 7 different robot platforms for pushing and pick&place tasks. The goal is to generalize robot controllers among different robot platforms. In addition, the work in [34] presents a large scale grasping dataset with multi robot platform, and in [35] a pushing dataset is introduced. To the best of our knowledge, there

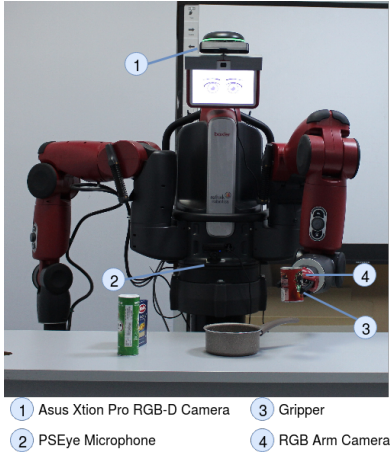


Fig. 2: Experimental environment

exists no publicly available multimodal dataset on robot manipulation failures. The dataset introduced in this work, as the first of its kind, rather focuses on the failed attempts of various robot manipulation actions (e.g. pushing, pouring, pick&place, etc) while collecting multimodal sensor readings such as image, depth, and audio waves.

III. METHOD

A. Setup and Data Collection

The experimental setup is presented in Fig. 2. We use a Baxter humanoid robot with the following equipments: a parallel gripper, an Asus Xtion Pro RGB-D camera mounted on head, a PSEye microphone mounted on lower torso and Baxter’s default RGB camera mounted on the left arm which is also used for the manipulation execution. The object sets used in the experiments are visualized in Fig. 3.

During data collection, the robot is tasked to execute a manipulation and all synchronized sensor readings (i.e., RGB/RGB-D image streams, audio waves) are then simultaneously logged. Based on the manipulation ontology introduced in [36], we selected the following 5 unique manipulation types: *push*, *pick&place*, *pour*, *place-in-container*, *put-on-top*. The distribution of the successful and failed trials for each manipulation type is presented in Table I. Sampled frames for each successful and failed actions are visualized in Fig. 4.

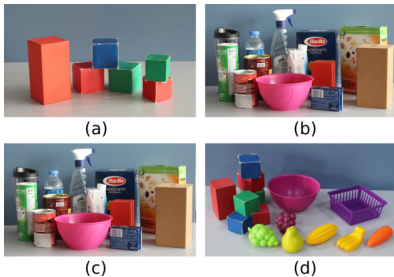


Fig. 3: Object sets for the (a) Pick&Place and Put-on-top, (b) Pushing, (c) Place-in-container, (d) Pouring manipulations.

TABLE I: Distribution of the successful and failed samples in our multimodal robot manipulation dataset.

Manipulation	#Successes	#Failures	Total
Push	12	19	31
Pick&place	13	32	45
Pour	25	42	67
Place-in-container	23	33	56
Put-on-top	9	21	30
	82	147	229

B. Data Preprocessing

The robot plans and executes trajectories online. The length of the recordings vastly vary due to executional differences in the manipulation and trajectory types. During manipulation, the scene might be partially observable or even non observable in some image frames due to the occlusions caused by the robot arm. To automatically eliminate such occluded frames, a depth-based thresholding method is applied. After filtering, remaining frames are roughly segmented into three phases corresponding to the *approach*, *manipulate* and *retreat* primitives, respectively. Next, we randomly sample four frames from each of *approach* and *retreat* primitives. Finally, for each sampled image, 224×224 pixels region of interest covering the table area is cropped. See Fig. 4 for randomly sampled 8 frames for each manipulation type.



Fig. 4: Sample successful and failed executions from the dataset.

C. Problem Description

In order to detect and reason about manipulation failures, the changes in the scene should be monitored using multiple sensory modalities [12] [11]. In this work, the failure detection task is modeled as a classification problem. Let there be $M \in \{1, 2, \dots\}$ sensing modalities where $m \in M$ is modality index. Let also D be the multimodal dataset where

$|D| = N$, x is observation, t_m is time index for modality m , i is recording index and $y \in \{success, fail\}$ is the class label:

$$D = \{ \{ (x_{1,i}^{(m)}, \dots, x_{t_m,i}^{(m)}) \}_{m=1}^M, y_i \}_{i=1}^N \quad (1)$$

The goal is to detect failures by learning a function $\Phi(\cdot)$ that maps multimodal sensory data to success or fail. For this purpose, we designed the following:

$$y = \Phi(\phi_1(x_1^{(1)}, \dots, x_{t_1}^{(1)}) \oplus \dots \oplus \phi_m(x_1^{(m)}, \dots, x_{t_m}^{(m)})) \quad (2)$$

where ϕ_m is unimodal convolutional neural network which acts as feature extractor, \oplus is the concatenation operator and Φ is the late fusion based classifier network.

To further identify the possible failure types, we also extend the experimental evaluation for the $|y| = 10$ case where successful and failed trials of each manipulation (i.e., 5 different types) are represented as individual classes.

D. FINO-Net

The proposed FINO-Net is a multimodal classifier network implemented not only to detect manipulation failures but also to classify observed failure types. The inputs of the network are composed of RGB and depth frames captured from head camera and audio waves recorded over the course of a robot manipulation. It adopts early fusion to combine RGB and depth frames and late fusion to combine vision and audio data. The architecture processes visual and audio inputs individually with a series of convolutional and convolutional-LSTM (convLSTM) layers. Finally, in the fusion step, the latent space representations are concatenated into a feature vector and fed to the fully connected layers. The overall FINO-Net architecture is depicted in Fig. 5. In the following subsections we elaborate more on the network architecture, loss function and training details.

1) *Vision*: In order to process spatio-temporal features in RGB and depth frames, we employ convLSTM cells. A typical LSTM cell is implemented using the fully connected layers, while a convLSTM replaces these with convolution operators. We use the following formulation:

$$i_t = \sigma(W_{xi} * x_t + W_{hi} * h_{t-1} + b_i) \quad (3)$$

$$f_t = \sigma(W_{xf} * x_t + W_{hf} * h_{t-1} + b_f) \quad (4)$$

$$o_t = \sigma(W_{xo} * x_t + W_{ho} * h_{t-1} + b_o) \quad (5)$$

$$g_t = \tanh(W_{xg} * x_t + W_{hg} * h_{t-1} + b_g) \quad (6)$$

$$c_t = f_t \cdot c_{t-1} + i_t \cdot g_t \quad (7)$$

$$h_t = o_t \cdot \tanh(c_t) \quad (8)$$

where $*$ and \cdot are the convolution and element-wise multiplication operators. The terms W and b represent the convolution weights and biases. The indices x and h define inputs and hidden state outputs, respectively.

The visual branch consists of three main blocks (see the top branch in Fig. 5). Inspired from [37], each block is composed of two convolutional layers and a convLSTM layer. RGB and depth frames are early fused by stacking

on top of each other before feeding to the first visual block. Inside each block, the filter numbers remain the same for all convolutional and convLSTM layers. Each convolutional layer has 3x3 filters. Before convLSTM layers, max pooling is applied to cut in half the number of features. Each block also has batch normalization and dropout layers.

2) *Audition*: In our earlier works [11], [12] we showed that audition can be employed to monitor manipulation execution as it provides complementary information to other sensing modalities. We also showed that Mel Frequency Cepstral Coefficients (MFCCs) are the suitable representations for auditory monitoring where Support Vector Machines were employed to classify audio features.

In this work, we adopt a convolutional network composed of two convolutional layers followed by a max pooling layer (see the bottom branch in Fig. 5). There are 64 filters in each layer with a filter size of 32. As input, we use single channel audio recordings with 16 KHz sampling rate. The raw audio signal is divided into 32 millisecond windows. For each window, Short Time Fourier Transform is applied to convert signal into frequency domain. Mel filterbank is applied and 20 MFCCs are obtained using librosa [38] library. The number of the audio windows are fixed by either applying padding or clipping.

3) *Fusion*: We adopt late fusion approach to combine visual and auditory modalities. In the fusion step, vision and audition features, obtained from final output of each modality, are concatenated into a single feature vector. The fusion layer is composed of two fully connected layers as shown in Fig. 5.

4) *Loss Function*: As shown in Table I, our dataset has imbalance between different failure classes. Such an imbalance in the training data makes the network to be more biased to the failure types that have more training samples, and thus leads to poor network performance [39]. To overcome the imbalance problem, we value more the under-represented failure samples by reinforcing the softmax cross-entropy loss with the smoothed frequency of each failure type as

$$\mathcal{L}(y, \hat{y}) = - \sum_i \alpha_i p(y_i) \log(p(\hat{y}_i)), \quad \alpha_i = 1/f_i \quad (9)$$

where y_i and \hat{y}_i are the true and predicted labels and f_i is the frequency, i.e. the sample number of the i^{th} failure.

5) *Optimizer And Regularization*: As an optimizer, we use Adam with a learning rate of 0.000001. Furthermore, batch normalization is applied after each convolutional layer. To boost the roles of very basic features (e.g. edges and curves), central dropout approach is adopted with the probability rate of 0.4. After each convolutional, convLSTM and fully connected layers a dropout layer is inserted except the first convolutional layer in Block 1 and the last convLSTM layer in Block 3.

To prevent overfitting, we augment the data by applying color augmentation and random flipping. For instance, the brightness, contrast, saturation, and hue values of all images in a sequence are randomly changed with a probability of 0.2.

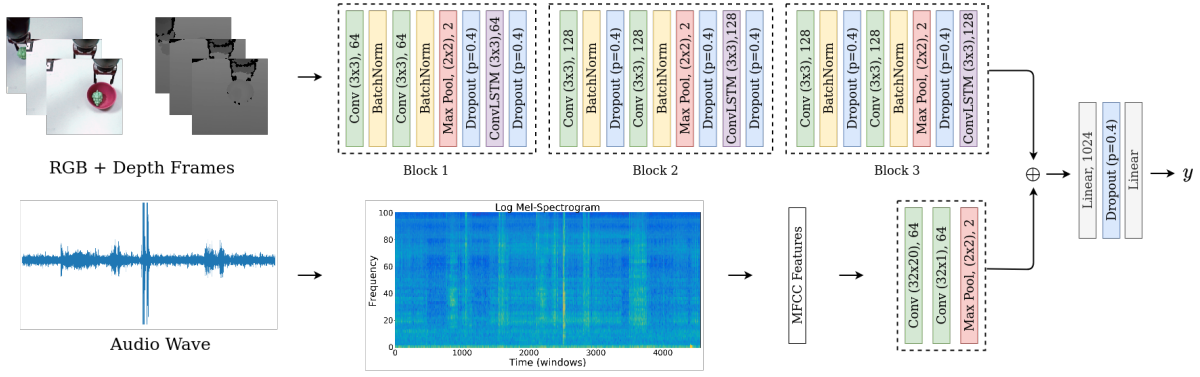


Fig. 5: FINO-Net Architecture

In similar fashion, each image sequence is flipped vertically with a probability of 0.5.

IV. EXPERIMENTS

We split our dataset into train (70%) and test (30%) sets by preserving the class distribution. Experimental results are presented in terms of class weighted precision, recall and F1-scores. Reported results are the highest scores obtained after applying early stopping. All experiments are conducted for both failure detection and identification cases, separately.

A. Baselines

We compare FINO-Net with a VGG-based network [40], which has 16 convolutional layers extended with an LSTM layer. The VGG baseline network is pretrained on ImageNet to be further used as a feature extractor. Obtained features from the final convolutional layer are fed into a single layer LSTM with 1024 neurons, followed by a fully connected layer. During training, only LSTM and fully connected layer weights are updated. For a fair comparison this baseline model is trained with the same parameters (e.g. learning rate, batch size, etc.) and the same strategy (e.g. loss function, data augmentation, etc.) used for the training of FINO-Net. Note that the baseline model is also extended with the same fusion structure that FINO-Net has. Following baseline networks are trained with the given modality data:

- VGG-RGB: The input of the network is only RGB frames obtained from head camera.
- VGG-D: The input is only single channel depth (D) frames captured from head camera.
- VGG-RGB-D: RGB and depth frames are stacked on top of each other to obtain 4 channel RGB-D input.
- VGG-RGB-D-A: Similar to FINO-Net, stacked RGB-D frames and audio (A) features are first individually processed and then are concatenated to be fed to the fully connected layer.

B. FINO-Net

To analyse the unique contribution of each sensing modality on the failure detection and identification tasks, we trained several variations of FINO-Net. To boost the performance, all convolutional and convLSTM layers of FINO-Net are initialized with the VGG weights pretrained on ImageNet. Next,

we perform various training operations with the following modality data from our proposed dataset:

- FINO-Net-RGB: Network is trained with only RGB input.
- FINO-Net-D: Network is trained with depth (D) frames only.
- FINO-Net-A: Only the audio (A) branch is trained. After the convolutional layers there is a single fully-connected layer with 64 neurons.
- FINO-Net-RGB-D: The visual branch of FINO-Net is trained by stacking RGB and depth frames as input to the network.
- FINO-Net-RGB-D-A: The entire network in Fig. 5 is trained with all the given modalities. The visual branch weights are initialized with FINO-Net-RGB-D and updated during training.

In addition to those experiments, we also freeze the FINO-Net weights initialized with that of the VGG baseline model. Next, our dataset is employed to train only the last convLSTM and the subsequent layers. Finally, the following experiments are performed:

- FINO-Net-F-RGB: While training the visual branch with RGB input, layers are frozen (F) except the final convLSTM and fully connected layers.
- FINO-Net-F-RGB-D: The vision branch is duplicated for RGB and depth frames. The RGB branch weights are frozen, except for the final convLSTM layer. All layers dedicated to the depth frames are updated. Next, RGB and depth features are concatenated and fed to the fully connected layers.
- FINO-Net-F-RGB-D-A: In addition to FINO-Net-F-RGB-D, audio features are concatenated with visual features before passing to the fully connected layers.

Note that in the experiments FINO-Net-F-RGB-D and FINO-Net-F-RGB-D-A, we treat the RGB and depth channels separately by duplicating the visual branch. This is because VGG features are learned from RGB ImageNet images and thus are not compatible with single-channel depth features. By updating the layers in the depth branch, we let the network explore unique depth cues which boost the network performance. This decoupling between the RGB and depth streams can also be interpreted as late fusion which is

different than the early fusion strategy employed in FINO-Net-RGB-D and FINO-Net-RGB-D-A.

C. Quantitative Results

When it comes to the baseline model VGG, we do not have the same observations: the depth modality (VGG-RGB-D) exhibits no contribution to the head camera data, i.e. VGG-RGB, in both failure detection and identification scenarios. The contribution of the audio modality is still less compared to the one observed in both FINO-Net models (FINO-Net-RGB-D-A and FINO-Net-F-RGB-D-A). These findings clearly show that our proposed FINO-Net has enough capacity to capture the unique contribution of each modality.

TABLE II: Quantitative Evaluation

	Push (S)	Push (F)	Place (S)	Place (F)	Put-In (S)	Put-In (F)	Put-On (S)	Put-On (F)	Pour (S)	Pour (F)
Push (S)	4	0	0	0	0	0	0	0	0	0
Push (F)	0	4	0	2	0	0	0	0	0	0
Place (S)	0	0	4	0	0	0	0	0	0	0
Place (F)	1	1	0	8	0	0	0	0	0	0
Put-In (S)	0	0	0	0	7	0	0	0	0	0
Put-In (F)	0	0	0	0	2	8	0	0	0	0
Put-On (S)	0	0	0	0	0	0	2	1	0	0
Put-On (F)	0	0	0	0	0	0	0	7	0	0
Pour (S)	0	0	0	0	0	0	0	0	7	1
Pour (F)	0	0	0	0	0	0	0	1	0	12

manipulation executions in a binary-classification manner. In the failure identification task, where the aim is to also distinguish the failure types, all models have certain accuracy drops since the number of classes increase from 2 to 10 (see sec. III-C). In this task, FINO-Net-F-RGB-D-A achieves a comparable performance (87.31%) with the baseline model (VGG-RGB-D-A) that reaches up to 88.89%.

V. CONCLUSION

Findings in Table II show that FINO-Net has enough capacity to capture unique contribution of each sensor modality, which is not the case for the baseline model. This plays a crucial role when the robot plans a recovery action to prevent such failures in time. For instance, the robot can autonomously decide what modality type(s) to rely on, in order to react to a failure with the most optimal action. In this regard, as a future work, we plan to employ the FINO-Net inferences, i.e. identified failure types, to help robot create an online recovery plan.

REFERENCES

- [1] C. Fritz, "Execution monitoring – a survey," University of Toronto, Tech. Rep., 2005.
- [2] O. Pettersson, "Execution monitoring in robotics: A survey," *Robotics and Autonomous Systems*, vol. 53, no. 2, pp. 73–88, 2005.
- [3] P. Goel, G. Dedeoglu, S. I. Roumeliotis, and G. S. Sukhatme, "Fault detection and identification in a mobile robot using multiple model estimation and neural network," in *IEEE Int. Conf. on Robotics and Automation (ICRA)*, vol. 3, 2000, pp. 2302–2309.
- [4] G. K. Fourlas, S. Karkanis, G. C. Karras, and K. J. Kyriakopoulos, "Model based actuator fault diagnosis for a mobile robot," in *IEEE Int. Conf. on Industrial Technology (ICIT)*, 2014, pp. 79–84.
- [5] D. Stavrou, D. G. Eliades, C. G. Panayiotou, and M. M. Polycarpou, "Fault detection for service mobile robots using model-based method," *Autonomous Robots*, pp. 1–12, 2015.
- [6] M. Ersen, E. Oztop, and S. Sariel, "Cognition-enabled robot manipulation in human environments: Requirements, recent work, and open problems," *IEEE Robotics Automation Magazine*, vol. 24, no. 3, pp. 108–122, 2017.
- [7] M. Kapotoglu, C. Koc, S. Sariel, and G. Ince, "Action monitoring in cognitive robots (in turkish)," in *Signal Processing and Communications Applications Conference (SIU)*, 2014, pp. 2154–2157.
- [8] D. Park, Y. Hoshi, and C. C. Kemp, "A multimodal anomaly detector for robot-assisted feeding using an lstm-based variational autoencoder," *Robotics and Automation Letters*, vol. 3, no. 3, pp. 1544–1551, 2018.
- [9] D. Park, H. Kim, and C. C. Kemp, "Multimodal anomaly detection for assistive robots," *Autonomous Robots*, vol. 43, no. 3, pp. 611–629, 2019.
- [10] I. Saltali, S. Sariel, and G. Ince, "Scene analysis through auditory event monitoring," in *Proceedings of the International Workshop on Social Learning and Multimodal Interaction for Designing Artificial Agents*. ACM, 2016, p. 5.
- [11] A. Inceoglu, G. Ince, Y. Yaslan, and S. Sariel, "Comparative assessment of sensing modalities on manipulation failure detection," in *IEEE ICRA Workshop on Perception, Inference and Learning for Joint Semantic, Geometric and Physical Understanding*, 2018.
- [12] A. Inceoglu, G. Ince, Y. Yaslan, and S. Sariel, "Failure detection using proprioceptive, auditory and visual modalities," in *IEEE/RSJ International Conference on Intelligent Robots and Systems (IROS)*. IEEE, 2018, pp. 2491–2496.
- [13] R. Chalapathy and S. Chawla, "Deep learning for anomaly detection: A survey," *arXiv preprint arXiv:1901.03407*, 2019.
- [14] J. Gertler, *Fault detection and diagnosis in engineering systems*. CRC press, 1998.
- [15] J. P. Mendoza, M. Veloso, and R. Simmons, "Focused optimization for online detection of anomalous regions," in *IEEE Int. Conf. on Robotics and Automation (ICRA)*, 2014, pp. 3358–3363.
- [16] J. P. Mendoza, M. Veloso, and Simmons, "Plan execution monitoring through detection of unmet expectations about action outcomes," in *ICRA*, 2015, pp. 3247–3252.
- [17] J. P. Mendoza, R. Simmons, and M. Veloso, "Detection and correction of subtle context-dependent robot model inaccuracies using parametric regions," *The International Journal of Robotics Research*, 2019.
- [18] R. Micalizio, "Action failure recovery via model-based diagnosis and conformant planning," *Computational Intelligence*, vol. 29, no. 2, pp. 233–280, 2013.
- [19] A. Bouguerra, L. Karlsson, and A. Saffiotti, "Handling uncertainty in semantic-knowledge based execution monitoring," in *IROS*, 2007, pp. 437–443.
- [20] P. Doherty, J. Kvarnstrom, and F. Heintz, "A temporal logic-based planning and execution monitoring framework for unmanned aircraft systems," *Autonomous Agents and Multi-Agent Systems*, vol. 19, no. 3, pp. 332–377, 2009.
- [21] S. Adam, M. Larsen, K. Jensen, and U. P. Schultz, "Towards rule-based dynamic safety monitoring for mobile robots," in *Simulation, Modeling, and Programming for Autonomous Robots*. Springer, 2014, pp. 207–218.
- [22] O. Pettersson, L. Karlsson, and A. Saffiotti, "Model-free execution monitoring in behavior-based robotics," *Trans. on Systems, Man, and Cybernetics, Part B: Cybernetics*, vol. 37, no. 4, pp. 890–901, 2007.
- [23] L. Mauro, F. Puja, S. Grazioso, V. Ntouskos, M. Sanzari, E. Alati, and F. Pirri, "Visual search and recognition for robot task execution and monitoring," *arXiv preprint arXiv:1902.02870*, 2019.
- [24] V. Sathish, M. Orkisz, M. Norrlof, and S. Butail, "Data-driven gearbox failure detection in industrial robots," *IEEE Transactions on Industrial Informatics*, 2019.
- [25] X. Zhou, H. Wu, J. Rojas, Z. Xu, and S. Li, *Nonparametric Bayesian Method for Robot Anomaly Monitoring*. Springer Singapore, 2020, pp. 51–93.
- [26] H. Wu, Y. Guan, and J. Rojas, "A latent state-based multimodal execution monitor with anomaly detection and classification for robot introspection," *Applied Sciences*, vol. 9, no. 6, p. 1072, 2019.
- [27] D. Ramachandram and G. W. Taylor, "Deep multimodal learning: A survey on recent advances and trends," *IEEE Signal Processing Magazine*, vol. 34, no. 6, pp. 96–108, 2017.
- [28] A. Eitel, J. T. Springenberg, L. Spinello, M. Riedmiller, and W. Burgard, "Multimodal deep learning for robust rgb-d object recognition," in *IROS*. IEEE, 2015, pp. 681–687.
- [29] A. Pieropan, G. Salvi, K. Pauwels, and H. Kjellstrom, "Audio-visual classification and detection of human manipulation actions," in *2014 IEEE/RSJ International Conference on Intelligent Robots and Systems*. IEEE, 2014, pp. 3045–3052.
- [30] D. Feng, C. Haase-Schutz, L. Rosenbaum, H. Hertlein, C. Glaeser, F. Timm, W. Wiesbeck, and K. Dietmayer, "Deep multi-modal object detection and semantic segmentation for autonomous driving: Datasets, methods, and challenges," *IEEE Transactions on Intelligent Transportation Systems*, 2020.
- [31] A. Mandlekar, Y. Zhu, A. Garg, J. Booher, M. Spero, A. Tung, J. Gao, J. Emmons, A. Gupta, E. Orbay *et al.*, "Roboturk: A crowdsourcing platform for robotic skill learning through imitation," in *Conference on Robot Learning*, 2018, pp. 879–893.
- [32] A. Mandlekar, J. Booher, M. Spero, A. Tung, A. Gupta, Y. Zhu, A. Garg, S. Savarese, and L. Fei-Fei, "Scaling robot supervision to hundreds of hours with roboturk: Robotic manipulation dataset through human reasoning and dexterity," in *IEEE/RSJ International Conference on Intelligent Robots and Systems (IROS)*, 2019, pp. 1048–1055.
- [33] S. Dasari, F. Ebert, S. Tian, S. Nair, B. Bucher, K. Schmeckpeper, S. Singh, S. Levine, and C. Finn, "Robonet: Large-scale multi-robot learning," in *CoRL 2019: Volume 100 Proceedings of Machine Learning Research*, 2019.
- [34] S. Levine, P. Pastor, A. Krizhevsky, J. Ibarz, and D. Quillen, "Learning hand-eye coordination for robotic grasping with deep learning and large-scale data collection," *The International Journal of Robotics Research*, vol. 37, no. 4–5, pp. 421–436, 2018.
- [35] C. Finn, I. Goodfellow, and S. Levine, "Unsupervised learning for physical interaction through video prediction," in *Advances in Neural Information Processing Systems (NeurIPS)*, 2016, pp. 64–72.
- [36] F. Worgotter, E. E. Aksoy, N. Kruger, J. Piater, A. Ude, and M. Tamasiunaite, "A simple ontology of manipulation actions based on hand-object relations," *IEEE Transactions on Autonomous Mental Development*, vol. 5, no. 2, pp. 117–134, 2013.
- [37] J. Rothfuss, F. Ferreira, E. E. Aksoy, Y. Zhou, and T. Asfour, "Deep episodic memory: Encoding, recalling, and predicting episodic experiences for robot action execution," *IEEE Robotics and Automation Letters*, vol. 3, no. 4, pp. 4007–4014, 2018.
- [38] B. McFee, C. Raffel, D. Liang, D. P. Ellis, M. McVicar, E. Battenberg, and O. Nieto, "librosa: Audio and music signal analysis in python," in *Python in Science Conference*, vol. 8, 2015, pp. 18–25.
- [39] E. E. Aksoy, S. Baci, and S. Cavdar, "Salsanet: Fast road and vehicle segmentation in lidar point clouds for autonomous driving," in *IEEE IV*, 2020.
- [40] K. Simonyan and A. Zisserman, "Very deep convolutional networks for large-scale image recognition," *Preprint arXiv:1409.1556*, 2014.